Magn Reson Med Sci 2018; 17; 95–99
doi:10.2463/mrms.cr.2016-0101
Published Online: February 13, 2017

CASE REPORT

Characteristics of Hepatic Schwannoma Presenting as an Unusual Multi-cystic Mass on Gadoxetic Acid Disodium-enhanced MR Imaging

Hiroki Haradome,[1*] Jun Woo,[1] Hisashi Nakayama,[2] Haruna N. Watanabe,[3] Masahiro Ogawa,[4] Mitsuhiko Moriyama,[4] Masahiko Sugitani,[3] Tadatoshi Takayama,[2] and Osamu Abe[5]

Hepatic schwannoma is a very rare hepatic tumor, usually appearing as a hypervascular solid mass with or without various degrees of cystic changes; however, to the best of our knowledge, only the two cases of hepatic schwannoma showing a multi-cystic appearance have previously been reported. We report herein a benign hepatic schwannoma presenting as an unusually large multi-cystic mass. The gadoxetic acid disodium-enhanced magnetic resonance imaging features are described with the histopathologic correlation and briefly review the literature. The solid-like areas showing the early/progressive enhancement, reflecting remnants of the Antoni A/B portion, during the dynamic phases may be helpful imaging features for the differentiation of other multi-cystic hepatic lesions, but pathological evaluation remains essential for diagnosis.

Keywords: *schwannoma, liver, magnetic resonance imaging, gadoxetic acid disodium*

Introduction

Schwannoma is a benign neurogenic tumor derived from Schwann cells; it may also be referred to as neurilemmoma, neuroma, neurinoma, and nerve sheath tumor. Theoretically, Schwannoma can occur in any nerve trunk or organ, except for the olfactory and optic nerves because they lack Schwann cells.[1] The most commonly affected sites include the upper extremities, trunk, head and neck, retroperitoneum, mediastinum, and pelvis.[2] Schwannomas have also been reported to occur in unusual locations, including the rectum, bile duct, and stomach;[2] however schwannomas arising from the liver are quite uncommon.

Hepatic schwannoma was first reported by Pereira et al in 1978,[3] and only 23 cases, of which 17 were benign and 6 were malignant, have been thus far reported in the English literature.[4–22] Pathologically, a schwannoma is characterized by a contexture of mixed Antoni A and B areas. Antoni A areas are hypercellular components that contain dense spindle cells in a nuclear palisade arrangement (palisading) and are supplied by profuse blood flow. In contrast, Antoni B areas are loose myxoid components with a few cells and a scarce blood supply. The relative proportions of the two components can vary between tumors, which can influence tumor appearance.

A schwannoma usually appears as an encapsulated solid mass with the various degrees of cystic and hemorrhagic degeneration, particularly in large lesions, which may mimic malignant neoplasms; however, schwannomas with a multi-cystic appearance are extremely unusual, and only two cases have been reported.[6,17]

We report herein a middle-aged woman with a benign hepatic schwannoma appearing as a large multi-cystic mass, describe its gadoxetic acid disodium (EOB)-enhanced MR imaging features with the correlation of the histopathology and briefly review the literature.

Case Report

A hepatic mass was incidentally noted by abdominal ultrasound during a regular check-up in a 50-year-old woman without symptoms. She was then referred to our hospital for further examination and treatment. She had a history of untreated diabetes mellitus and gallstones, but no history of hepatic disorders. She did not have either a drinking or smoking habit. Physical examination revealed no remarkable findings, such as a

[1]Department of Radiology, Nihon University School of Medicine, 30-1, Ohyaguchi Kamicho, Itabashi, Tokyo 173-8610, Japan
[2]Department of Digestive Surgery, Nihon University School of Medicine, Tokyo, Japan
[3]Department of Pathology, Nihon University School of Medicine, Tokyo, Japan
[4]Department of Gastroenterology, Nihon University School of Medicine, Tokyo, Japan
[5]Department of Radiology, Graduate School of Medicine, The University of Tokyo, Tokyo, Japan

*Corresponding author, Phone: +81-3-3972-8111, Fax: +81-3-3958-2454, E-mail: karate.b@gmail.com

Received: September 18, 2016 | Accepted: December 7, 2016

palpable abdominal mass, abdominal tenderness, or abnormal bowel sounds. Routine hematological and blood biochemistry examination results were normal. All hepatitis B and C virus-related indices were negative. The cancer antigen 19-9 level was slightly elevated (46.8 U/mL); however, the levels of other tumor markers, including alpha-fetoprotein, protein induced by vitamin K absence or antagonist-II, and carcinoembryonic antigen, were within normal limits.

Contrast-enhanced CT evealed a large, well-defined multi-cystic mass with a maximum diameter of 7.8 cm in the left hepatic lobe; some nodular arterial enhancement areas that persisted until the equilibrium phase were observed along the septa. A moderately enhanced thin capsule surrounding the mass was also identified at equilibrium phase on contrast-enhanced dynamic CT. The mass had mixed loculi showing water density and slight hyperdensity, suggesting hemorrhage on plain CT. Neither calcification nor fat components were observed in the mass. No lymph node swelling or lesions in other organs were observed.

On MR imaging, a multi-cystic mass with a thin capsule showing heterogeneous hyperintensity on both fat-saturated T_2-weighted (TR/TE, 4498/97.9 ms; matrix, 320 × 22; slice thickness/gap, 7/8.4 mm) (Fig. 1A) and diffusion-weighted (TR/TE, 14117.6/67.3 ms; matrix, 128 × 160; slice thickness/gap, 7/8.4 mm; b-value, 1000 s/mm^2) (Fig. 1B) images was observed in the left lobe. Some loculi of the mass showed hyperintensity on precontrast fat-saturated T_1-weighted (LAVA: TR/TE, 4.96/2.15 ms; flip angle, 12 degree; matrix, 320 × 224; slice thickness/gap, 3.6/1.8 mm) (Fig. 1C) imaging reflecting hemorrhage, and some of them contained fluid-fluid levels on fat-saturated T_2-weighted imaging due to plasma-blood separation (hematocrit effect) (Fig. 1A). On EOB-enhanced MR images (Fig. 1D–G), some nodular arterial enhanced areas and several gradually enhanced solid-like areas along the septa were observed during the dynamic phases; they also showed slight hypointensity at the hepatocyte phase on 15 min. In contrast, the cystic parts appeared as clearly more hypointense areas compared to the solid-like parts at the hepatocyte phase. However, on T_2-weighted and diffusion-weighted images, the solid-like and cystic parts were difficult to distinguish from each other because they appeared to be similarly hyperintense. The mass was primarily located at segment 4 and protruded toward the hepatic hilum (Fig. 1H). Mild intrahepatic duct dilatation was observed at the periphery of the mass due to its compression, but no fat component was identified in the mass.

Based on these imaging findings, mucinous cystic neoplasm (MCN), cyst-forming intraductal papillary neoplasm of the bile duct (IPNB), hydatid disease, and degenerated schwannoma were considered as the differential diagnosis. However, mesenchymal sarcoma could not be excluded; left lobectomy was planned to determine the pathology.

Macroscopically, the resected tumor appeared as an encapsulated yellowish mass, measuring 7.8 cm in maximum diameter; it had a multi-cystic appearance with multiple septa at the cut surface (Fig. 2A). Hematoxylin-eosin–stained sections revealed mixed dense and loose spindle cell proliferation separated by multiple septa and extensive cystic and hemorrhagic degenerated areas (Fig. 2B). The spindle cells appeared in a nuclear palisade arrangement (palisading), corresponding to Antoni A areas (Fig. 2C). The majority of the tumor consisted of myxoid components with loose spindle cell proliferation (Antoni B areas) and several cystic and hemorrhagic areas. No significant evidence of nuclear atypia,

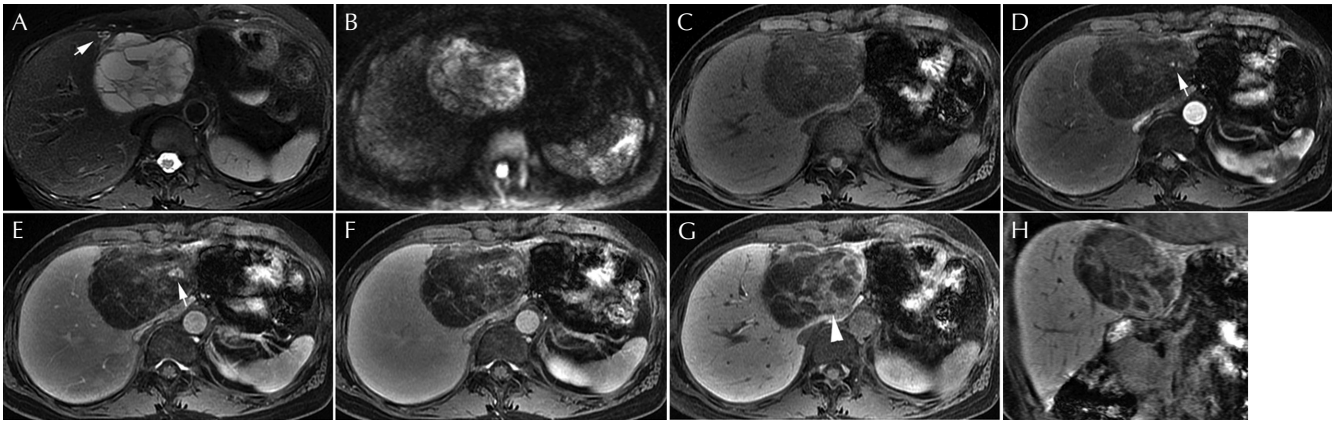

Fig. 1 Plain and EOB-enhanced MR images. (**A**) Fat-saturated T_2-weighted and (**B**) diffusion-weighted (b-value = 1000 s/mm^2) images demonstrate a heterogeneous hyperintense multi-cystic mass with a thin capsule. Some loculi of the mass show hyperintensity on (**C**) pre-contrast fat-saturated T_1-weighted imaging reflecting hemorrhage, and some of them reveal fluid-fluid levels on (**A**) fat-saturated T_2-weighted imaging due to plasma-blood separation. (**D**–**G**: **D**, arterial phase [32 sec]; **E**, portal phase [70 sec]; **F**, late phase [180 sec]; **G** and **H** hepatocyte phase [15 min]). Gadoxetic acid disodium-enhanced MR images show some nodular arterial enhanced areas (arrows) and several gradually enhanced solid-like areas along the septa (arrowhead) during dynamic phases (**D**–**F**), and they showed slight hypointensity at the hepatocyte phase (**G**). The mass was primarily located at segment 4 and protruded toward the hepatic hilum (**H**). Mild intrahepatic duct dilatation (arrow) is also observed at the periphery of the mass (**A**). Notably, the cystic part appears as a clearly more hypointense area compared to the solid-like part at the hepatocyte phase (**G**), although the solid-like and cystic parts are similarly hyperintense on fat-saturated T_2-weighted (**A**) and diffusion-weighted images (**B**).

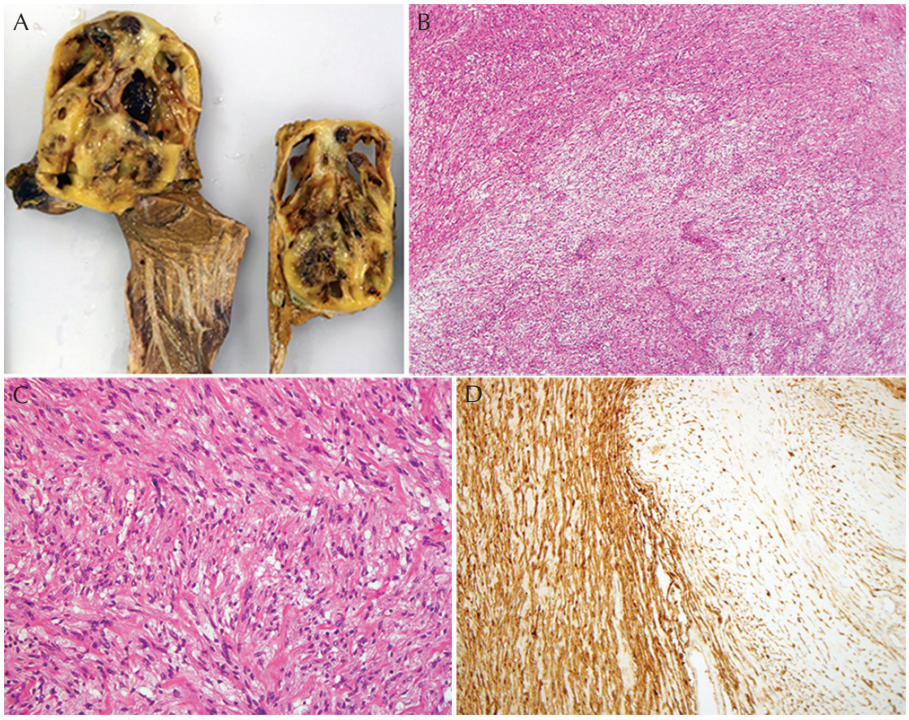

Fig. 2 Macroscopic, microscopic, and immunohistochemical staining features. (**A**) Macroscopically, the resected tumor appeared as an encapsulated multicystic yellowish-white mass with multiple septa. (**B**) A low-power photomicrograph (hematoxylin-eosin [H-E stain]; magnification, x4) demonstrated mixed density and loose spindle cell proliferation, separated by multiple septa and extensive cystic and hemorrhagic degenerated areas. The majority of the tumor consisted of myxoid components with loose spindle cell proliferation (Antoni B areas) and several cystic and hemorrhagic areas. (**C**) A high-power photomicrograph (H-E stain; magnification, x20) revealed that the spindle cells showed a nuclear palisade arrangement, corresponding to Antoni A areas. (**D**) Immunohistochemistry (magnification, x10) revealed the tumor cells are diffusely positive for S-100 protein.

mitosis, or necrosis was apparent. The tumor was surrounded by normal hepatic parenchyma. No infiltrative growth or vessel invasion was observed. The margin of the resected mass contained no tumor cells. Immunohistochemical staining indicated that the tumor cells were positive for S-100 protein (Fig. 2D) but were negative for neurofilaments.

Based on these histological findings, a final diagnosis of benign hepatic schwannoma was pathologically confirmed. The postoperative course was uneventful and no signs of local recurrence have been observed in the patient so far.

Discussion

Schwannoma is an encapsulated, slow-growing, neurogenic tumor derived from the Schwann cells of the peripheral nerve. Schwannoma can occur anywhere in the nerve trunk or organs; however, it very rarely arises in the liver, presenting as hepatic schwannoma.

Schwannoma is also associated with neurofibromatosis in approximately 50% of the cases, and three such cases of hepatic schwannoma have been reported;[8,20,21] however, the present case did not appear to have associated neurofibromatosis. In extremely rare cases, these tumors can cause malignant transformation, even in hepatic schwannoma; six malignant hepatic schwannomas have been reported to date.[9–11,20–22]

The sympathetic and parasympathetic fibers originating from the hepatic plexus in the liver hilum, some of which are also distributed among the interlobular connective tissues along the portal veins and arteries, are thought to be the origin of hepatic schwannomas.[23] In general, schwannomas can occur at any age, but primarily arise in patients aged 20–50 years, with no differences between genders. The results of a 40-year review of previously reported hepatic schwannomas by Wan et al.[4] revealed a mean age of 51.7 years (range, 21–83 years), which is not too different from that of all schwannomas; however, more hepatic schwannoma patients tend to be female, as is the present patient. These investigators[4] also reported that hepatic schwannomas were more common in Asians than in Europeans and North Americans.

The major symptoms of patients with hepatic schwannoma are upper abdominal pain/discomfort, as described previously; however, several patients without any symptoms have recently been reported, because hepatic masses are increasingly being found incidentally on routine or follow-up imaging due to advanced imaging modalities. Patients with malignant schwannomas rarely complain of obstructive jaundice, and there is no case of patients with benign schwannomas and obstructive jaundice.[4]

The tumor size in the reported cases varied between 2.3 and 30 cm. Malignant tumors tended to be larger (mean, 16.7 cm), although some benign tumors were also large (>20 cm in diameter), as in the present case. Tumors have been observed in all lobes, although benign lesions occurred predominately in the right lobe, while the left or both lobes were affected in malignant cases.[4]

Hepatic schwannomas usually appear as hypervascular solid masses with or without various degree of cystic changes; however, they may show various morphology depending on the ratio of Antony A and B areas and/or secondary degeneration including cystic changes, hemorrhage, necrosis, and calcification, which may be misdiagnosed as liver metastasis from gastrointestinal stromal tumor or breast

cancer, intrahepatic cholangiocarcinoma, or mesenchymal tumor on primary diagnosis.[4]

To our knowledge, among the 23 reported cases of hepatic schwannoma in the English literature,[4–22] only two cases of benign hepatic schwannoma appeared as multi-cystic masses,[6,17] as in the present case. Both of these reported cases were preoperatively misinterpreted as hepatic hydatid cyst based on primary examination. Both patients were female, and the tumors were located in the right hepatic lobe. Both tumors were associated with secondary cystic degeneration, which contributed to a multi-cystic appearance. No precise descriptions of the imaging features, such as a tumor contrast-enhancement patterns, were included in the two previous reports, and in addition, no data regarding MR imaging features have been reported. In the present case, MR imaging showed a multi-cystic mass with a thin capsule and some loculi showing hyperintensity on fat-saturated T_1-weighted imaging, reflecting hemorrhage within the mass (Fig. 1A–C). An EOB-enhanced MR image depicted some arterially enhanced nodular areas and several gradually enhanced solid-like areas along the septa during the dynamic phases, and they became slightly hypointense at the hepatocyte phase (Fig. 1D–G). In contrast, the cystic parts clearly showed more hypointensity than the solid-like part at the hepatocyte phase (Fig. 1G, H). Based on the histopathological-imaging correlation, the arterial nodular enhancement and gradually enhanced solid-like areas during the dynamic phases corresponded primarily to Antoni A and Antoni B components, respectively. The slightly hypointense solid-like areas at the hepatocyte phase corresponded to both Antoni A and B components, but both the solid-like areas and cystic parts appeared to be similarly hyperintense on T_2-weighted and diffusion-weighted images because regions corresponding to solid-like areas contained a predominantly myxoid component (Antoni B). Thus, the hepatocyte phase of EOB-enhanced MR image may depict solid-like part including abundant myxoid component and cystic part as each different signal area due to paradoxical uptake of EOB in solid-like part, which is presumed to be attributed to interstitial diffusion of the contrast within the area of myxoid component. In the present case, massive cystic degeneration and hemorrhage were noted in the Antoni B areas, which were assumed to result from vascular thrombosis and subsequent necrosis.[4]

The major differential diagnoses for hepatic schwannoma showing an unusual multi-cystic appearance include hepatic hydatid cyst (hydatid disease), MCN, and cyst-forming IPNB. Hydatid disease is a parasitic disorder caused by Echinococcus infection that is endemic in various regions of the world, including the Mediterranean, Africa, South America, the Middle East, Australia, and New Zealand. Hydatid disease can occur anywhere in the body. The liver is the most frequent site of involvement; it appears as solitary or multiple multi-cystic mass lesions, and calcification is more common in hepatic hydatid cysts. However, in these cysts, no enhanced solid parts or hemorrhagic areas within the lesion are observed, in contrast to hepatic schwannoma.[24] In addition, a diagnosis of hepatic hydatid cyst may be given less consideration in non-immigrants or persons without a history of travel to endemic regions. Cyst-forming IPNB is also considered in the differential diagnosis, because it can form solitary multi-cystic hepatic masses and is relatively frequently accompanied by mildly enhanced mural nodules. The characteristic findings of IPNB include a multi-cystic mass with a grape-like appearance, communication with the bile ducts, bile duct dilatation, and papillary projections into the bile duct.[25] These findings are helpful for suggesting cyst-forming IPNB. Finally, MCN, which is defined as a cyst-forming epithelial neoplasm with ovarian-like stroma and has formerly been classified as biliary cystadenoma or biliary cystadenocarcinoma, can closely resemble a hepatic schwannoma with a multi-cystic appearance. MCN occurs almost exclusively in females and appears as a well-defined multi-cystic mass (cyst-in-cyst appearance) with a capsule.[26] Moreover, MCN is sometime associated with hemorrhage and calcification.[26] However, in MCN, enhanced solid regions are less frequently seen, because the majority of MCNs show a benign or borderline malignant pathology.[26] Therefore, early and/or gradually enhanced solid-like areas reflecting remnants of the Antoni A /B portion may be helpful for distinguishing the two tumors, although imaging discrimination still appears to be extremely challenging and pathological diagnosis remains essential for diagnosis.

In summary, hepatic schwannoma should be considered as a differential diagnosis for multi-cystic hepatic masses, although it may have an unusual appearance. The solid-like areas showing early/progressive enhancement areas, reflecting remnants of the Antoni A/B portion, during the dynamic phases may be helpful imaging features for the differentiation of other multi-cystic hepatic lesions, but pathological evaluation remains essential for diagnosis. The hepatocyte phase of EOB-enhanced MR image may depict solid-like part including abundant myxoid component and cystic part as each different signal area due to the paradoxical uptake of EOB in solid-like part, which is presumed to be attributed to the interstitial diffusion of the contrast within an area of myxoid component (Antoni B).

Conflicts of Interest

The authors declare that they have no conflicts of interest.

References

1. Kulkarni N, Andrews SJ, Rao V, Rajagopal KV. Case report: Benign porta hepatic schwannoma. Indian J Radiol Imaging 2009; 19:213–215.
2. Yu RS, Sun JZ. Pancreatic schwannoma: CT findings. Abdom Imaging 2006; 31:103–5.
3. Pereira Filho RA, Souza SA, Oliveira Filho JA. Primary neurilemmal tumour of the liver: case report. Arq Gastroenterol 1978; 15:136–138.

4. Wan DL, Zhai ZL, Ren KW, Yang YC, Lin SZ, Zheng SS. Hepatic schwannoma: A case report and an updated 40-year review of the literature yielding 30 cases. Mol Clin Oncol 2016; 4:959–964.
5. Hytiroglou P, Linton P, Klion F, Schwartz M, Miller C, Thung SN. Benign schwannoma of the liver. Arch Pathol Lab Med 1993; 117:216–218.
6. Ozkan EE, Guldur ME, Uzunkoy A. A case report of benign schwannoma of the liver. Intern Med. 2010; 49:1533–1536.
7. Ota Y, Aso K, Watanabe K, et al. Hepatic schwannoma: imaging findings on CT, MRI and contrast-enhanced ultrasonography. World J Gastroenterol 2012; 18: 4967–4972.
8. Heffron TG, Coventry S, Bedendo F, Baker A. Resection of primary schwannoma of the liver not associated with neurofibromatosis. Arch Surg 1993; 128:1396–1398.
9. Iddings DM, Wright BE, Bilchik A. A rare cause of primary hepatic neoplasm: malignant peripheral nerve sheath tumor in the age of modern liver surgery. Am Surg 2008; 74:47–50.
10. Kóbori L, Nagy P, Máthé Z, et al. Malignant peripheral nerve sheath tumor of the liver: a case report. Pathol Oncol Res 2008; 14:329–332.
11. Morikawa Y, Ishihara Y, Matsuura N, Miyamoto H, Kakudo K. Malignant schwannoma of the liver. Dig Dis Sci 1995; 40:1279–1282.
12. Wada Y, Jimi A, Nakashima O, Kojiro M, Kurohiji T, Sai K. Schwannoma of the liver: report of two surgical cases. Pathol Int 1998; 48:611–617.
13. Akin M, Bozkirli B, Leventoglu S, et al. Liver schwannoma incidentally discovered in a patient with breast cancer. Bratisl Lek Listy 2009; 110:298–300.
14. Hayashi M, Takeshita A, Yamamoto K, Tanigawa N. Primary hepatic benign schwannoma. World J Gastrointest Surg 2012; 4:73–78.
15. Kapoor S, Tevatia MS, Dattagupta S, Chattopadhyay TK. Primary hepatic nerve sheath tumor. Liver Int 2005; 25: 458–459.
16. Yoshida M, Nakashima Y, Tanaka A, Mori K, Yamaoka Y. Benign schwannoma of the liver: a case report. Nihon Geka Hokan 1994; 63:208–214.
17. Flemming P, Frerker M, Klempnauer J, Pichlmayr R. Benign schwannoma of the liver with cystic changes misinterpreted as hydatid disease. Hepatogastroenterology 1998; 45:1764–1766.
18. Momtahen AJ, Akduman EI, Balci NC, Fattahi R, Havlioglu N. Liver schwannoma: findings on MRI. Magn Reson Imaging 2008; 26:1442–1445.
19. Lee WH, Kim TH, You SS, et al. Benign schwannoma of the liver: a case report. J Korean Med Sci 2008; 23: 727–730.
20. Young SJ. Primary malignant neurilemmona (schwannoma) of the liver in a case of neurofibromatosis. J Pathol 1975; 117:151–153.
21. Lederman SM, Martin EC, Laffey KT, Lefkowitch JH. Hepatic neurofibromatosis, malignant schwannoma, and angiosarcoma in von Recklinghausen's disease. Gastroenterology 1987; 92:234–239.
22. Fiel MI, Schwartz M, Min AD, Sung MW, Thung SN. Malignant schwannoma of the liver in a patient without neurofibromatosis: a case report and review of the literature. Arch Pathol Lab Med. 1996; 120:1145–1147.
23. Northover JM, Terblanche J. A new look at the arterial supply of the bile duct in man and its surgical implications. Br J Surg 1979; 66:379–384.
24. Polat P, Kantarci M, Alper F, Suma S, Koruyucu MB, Okur A. Hydatid disease from head to toe. Radiographics 2003; 23:475–494.
25. Lim JH, Zen Y, Jang KT, Kim YK, Nakanuma Y. Cyst-forming intraductal papillary neoplasm of the bile ducts: description of imaging and pathologic aspects. AJR Am J Roentgenol 2011; 197:1111–1120.
26. Zen Y, Pedica F, Patcha VR, et al. Mucinous cystic neoplasms of the liver: a clinicopathological study and comparison with intraductal papillary neoplasms of the bile duct. Mod Pathol 2011; 24:1079–1089.